February 26, 2005, Version 1.3

# Multifractality of the US Treasury Term Structure and Fed Funds Rate


**Abstract**

This paper identifies the Multifractal Models of Asset Return (MMARs) from the eight nodal term structure series of US Treasury rates as well as the Fed Funds rate and, after proper synthesis, simulates those MMARs. We show that there is an inverse persistence term structure in the sense that the short term interest rates show the highest persistence, while the long term rates are closer to the GBM's neutral persistence. The simulations of the identified MMAR are compared with the original empirical time series, but also with the simulated results from the corresponding Brownian Motion and GARCH processes. We find that the eight different maturity US Treasury and the Fed Funds rates are multifractal processes. Moreover, using wavelet scalograms, we demonstrate that the MMAR outperforms both the GBM and GARCH(1,1) in time-frequency comparisons, in particular in terms of scaling distribution preservation. Identified distributions of all simulated processes are compared with the empirical distributions in snapshot and over time-scale (frequency) analyses. The simulated MMAR can replicate all attributes of the empirical distributions, while the simulated GBM and GARCH(1,1) processes cannot preserve the thick-tails, high peaks and proper skewness. Nevertheless, the results are somewhat inconclusive when the MMAR is applied on the Fed Funds rate, which has globally a mildly anti-persistent and possibly chaotic diffusion process completely different from the other nodal term structure rates.



Sutthisit Jamdee and Cornelis A. Los
Kent State University,
Department of Finance, Kent,
OH 44242-0001.
Email: clos500@cs.com and sjamdee@kent.edu

# 1 Introduction

Interest rates form some of the most important variables in finance. A change in interest rates usually has a substantial impact on an asset investments and derivatives pricing. Therefore there is considerable demand for well-identified interest rate models. The current discussion about interest rate models can be summarized as follows. Most financial market models consist of an affine (= "linear + intercept") mathematical system driven by a particular exogenous information process. Most information processes thus far assumed are either i.i.d. processes in discrete-time Wold-type models, or Wiener-Gauss processes in continuous time models. However, very recently the mono- and multi-fractal information processes of Mandelbrot have again become popular, after their initial popularity in the late 1960s and early 1970s. In addition, there is some discussion of nonlinear continuous time models driven by Wiener-Gauss processes (See, for example, Franke, Stapleton and Subrahmanyam, 1999). In this paper we will discuss the affine models driven by i.i.d./Wiener-Gauss and by fractal information processes and leave the comparison with the nonlinear models driven by i.i.d./Wiener-Gauss information processes for another paper.

The very first interest rate model, known as the one-factor affine model, or simple linear model with intercept, driven by an i.i.d. information process, was introduced by Vasicek (1977). Since then several models, ranging from very simple to very complex, in terms of the number of factors or information processes employed, have been proposed. Such one- or two-factor models of interest rate are preferred, since they can succinctly explain most of the variation of the term structure of interest rates. Most of these simple factor models assume a geometric Brownian motion (GBM) with a trend as their price diffusion process. This is not a coincidence, since it is imperative for transparency and scientific logic that the proposed models are tractable. In addition, sophisticated investors prefer the GBM, as many are already familiar with it from the Black-Scholes options pricing formula.

But accumulating evidence in the academic financial literature indicates that these GBMs

cannot explain several features of the empirical financial data. Already in 1970 Roll studied the distribution of the Treasury bill yield changes using the stability index, or Zolotarev-$\alpha_Z$, and found that "With a large degree of confidence, most of the distributions of interest rate changes have $\alpha$ significantly lower than 2 and are thus non-Gaussian Indeed, the upper limit of the simulation range suggests that most of the $\alpha$'s are significantly lower than 1.5" (p. 73). The GBM has a stability index equal to 2, or, what is the same, a Hurst exponent equal to the Fickian value of 0.5. Thus the characterizing feature of the GBM is that it scales the instantaneous volatility of pricing processes according to $\tau^{0.5}$, the square root of the maturity or time horizon $\tau$. This scaling characteristic can greatly affect actual derivatives prices when the underlying asset prices do not adhere to such time-frequency scaling (*e.g.*, Jamdee and Los, 2005).

Following Engle's (1982) Auto-regressive Conditional Heteroskedasticity or ARCH model, Bollerslev (1986) proposed the Generalized ARCH or GARCH model to explain the empirically observed time-varying volatility of financial market pricing processes, driven by i.i.d. information processes. But the users of the GARCH model experience serious difficulties with attempting to identify its proper lag orders. Practically, the GARCH (1, 1) is now very common in time series modeling, but that is mainly due to its overreaching simplicity. Although they capture skewness and kurtosis phenomena in addition to time-varying volatility, the GARCH models do not identify other important characteristics of empirical financial data, such as time-and-frequency scaling and long-range dependence, or "Long Memory".

To overcome the drawbacks of both the GBM and GARCH(1, 1) models, this paper uses the Multifractal Model of Asset Return (MMAR) of Calvet, Fisher and Mandelbrot (1997) as a viable and empirically more satisfying substitute to model each of the nine interest rates of the US term structure. In effect, we propose a nine-factor model, where each of the nodal interest rates is a multifractal Brownian motion, which is driven by a multifractal information process.

We implement the MMAR for the first time as the underlying process of the U.S. Treasury interest rate series for various maturities and compare its performance with that of the affine GBM

and GARCH models. Monte Carlo simulations are used for model performance measurement, in the sense that we want to ensure that the identified models can reproduce the identified characteristics of the interest rate series. It should be recognized that this study does not attempt to price any bonds. Rather, the study focuses on the analysis of simulated fractal price diffusion processes of the nodal market interest rates.

The main findings of this paper are that the interest rate series from the instantaneous to 10-year maturities exhibit Long Memory and scale over frequency and time. Our simulations of the empirically identified model suggest that the MMAR is superior to the GBM and GARCH(1, 1) processes in modeling the time-scaling characteristics of the interest rate series, while it maintains other desirable characteristics, like the tractability and heteroskedastic time-varying volatility of both these models.

The paper is organized as follows. Section 2 reviews the literature about interest modeling based on GBM and GARCH processes and enumerates their shortcomings which we try to overcome. Section 3 explains the empirical data. Section 4 explains the MMAR methodology used. It discusses how to detect multifractality, to identify the crucial parameters of the return series, to reconstruct the series using the identified parameters, to simulate the return process, to measure the model's overall performance, and to analyze the higher moments of the simulated results. Section 5 presents the empirical results and section 6 provides a summary and conclusions.

## 2 Literature Review

The very first interest rate model, a one-factor affine model, was introduced by (1977). Other popular affine models include the two-factor model of Longstaff and Schwartz (1992) and the one-factor model of Hull and White (1993). In particular, the two-factor model followed the introduction of the extended Vasicek and extended Cox, Ingersöll, and Ross (CIR) one-factor affine models. The one-factor model can only explain parallel (up-and-down) shifts of the term

structure of interest rates. The two-factor model can explain both its parallel and slope shifts.

The next generation of three-factor affine models, was proposed by Balduzzi *et al.* (1996). Based on the principal components analysis of the covariance matrix of interest rates, Brandt and Kavajecz (2004) suggest that more than one, but not many more than three factors, can sufficiently capture the parallel and slope and curvature changes of the term structure, *i.e.*, more than 90% of the term structure variation.

Besides assuming the GBM as the underlying interest rate diffusion process, some have tried to use the GARCH process as the underlying process, *e.g.*, Longstaff and Schwartz (1992). The following sections review the drawbacks of the affine GBM and GARCH(1, 1) processes, which leads us to a need for a better stochastic process for future development in interest rate modeling.

## 2.1 Limitation of the Affine Models

Los (1989, 2003) and Rebonato and Cooper (1996) argue that the statistical pitfalls of the principal component analysis to identify the factors for the models create a serious model identification problem. The percentage of variation attributable to a particular component depends on the number of components prejudicially retained from the covariance matrix. Thus, both the size of the covariance matrix, or the number of the term structure's maturity segments, as well as how many of these segments are considered significant, are crucial choices since these choices determine the percentages of variation decomposition. In fact, this problem is inherent to all more-than-one-factor affine models.

We mentioned that the one-factor Vasicek model only allows for parallel shifts of the term structure (Schlögl & Sommer, 1998). In addition, Bakshi and Chen (1996) and Rogers (1996) comment that with its assumed Gaussian distribution, the model can erroneously produce negative interest rates.

Cox *et al.* (1985) solve this problem by incorporating a reflecting boundary for the diffusion process. The resulting pricing process remains the same (an exponentially affine pricing process)

after their adjustment, although the new bond prices (= horizon dependent deterministic functions) are different. Schlögl and Sommer (1998) also argue that while the two-factor models allow for the twists or slopes of the term structure, they still do not generate the correct third and higher order dynamic distribution moments. Kappi (1997) uses maximum likelihood estimation (which can be shown to be equivalent to the scientifically deficient principal components analysis) to estimate the two-factor models and found that they can identify the level and the slope, but, unsurprisingly, cannot identify the curvature of the term structure. With one additional factor to explain the curvature, the three-factor models perform better than the two-factor models. However, Los (1989) and Brandt and Kavajecz (2004) clearly show that the three factors of those three-factor models are typically not uniquely identified, even though modelers commonly think of them as the level, slope, and curvature of the term structure.

While Duffie and Kan (1994) and Dai and Singleton (2000) correctly state that a price process that is exponentially linear in the short rate price process with drift and variance components in the one or two factors are features of the general class of affine models, these simple features are incompatible with the empirical evidence and do not correctly identify the time-varying distributional stucture of the term stucture's rates.

Johannes (2004) has recently tested both nonparametric one-factor models and the two- and three-factor models of Andersen and Lund (1997, 1998). The results indicate that none of these models are able to capture the ARCH and non-Gaussian long-term dependence ("scaling") features of the empirical data. Johannes (2004) argues that a multi-factor model might be able to match the nonlinearity of the observed data by grossly increasing the volatility in the model. However, the cost of the modification is so severe that the simulated interest rate path becomes completely irregular.

Thus the affine models fail correct empirical identification by the simple fact that the information structure of the model is generated by connecting a simple affine (= "linear") stucture and a (Fickian) GBM infomation process, that does not allow any singularities or exceptional,

unpredictable surprises, *i.e.*, the features that are empirically normally found in the financial markets.

## 2.2 GARCH Process Models

Bollerslev (1986) introduced the GARCH $(p, q)$ process, generalizing the 2003 Nobel Memorial Prize winning ARCH process of Engle (1982). The GARCH $(p, q)$ process has been found to be very useful in modeling the time-varying price volatility of underlying assets, *i.e.*, they are non-stationary in the weak sense and they are now widely accepted among academicians and practitioners.

Although GARCH can be used in any higher order of Moving Average and Autoregressive models, in practice only GARCH (1, 1) is widely used, because the paametes of higher-order GARCH models are vey difficult to uniquely identify and often have to be subjectively calibrated. Andersen and Lund (1997), Dai and Singleton (2000) use GARCH to approximate a density of short-rate series and then estimate their underlying processes. Without pricing any interest rate options, Brenner *et al.* (1996) suggest that GARCH model can capture stochastic volatility and varying serial correlation of the short-rate, the 3-month Treasury bill, series.

Longstaff and Schwartz (1992) also use GARCH to capture the underlying process of the short rate in their two-factor model, but later found that their model inadequately reproduces reality. Fisher *et al.* (1997) argue that the finite memory of the discrete time GARCH process prevents it from replicating the long memory time-and-frequency scaling patterns found in empirical financial market data.

Imposing multi-factor interest rate models on a GARCH information process to capture either the short-rate process or its volatilities, Bali (2003), Heston and Nandi (2003), and Saltoglu (2003) show that GARCH helps improve the predictability of multi-factor models, although Saltoglu (2003) reports that GARCH model is slightly outperformed by other nonparametric methods such as (nonlinear) Artificial Neural Networks and kernel smoothing.

The limitations of the GARCH model, such as its the unidentifiable lag orders and its finite short term memory, urge us to find a better identified model. One of the currently most promising models is the MMAR.

## 2.3 Multifractality Modeling

The MMAR is the third generation of price diffusion models, following the multifractality theory of Mandelbrot (Mandelbrot and Hudson, 2004). This model is based on the compounding of a (Fickian) geometric Brownian motion interest rate pricing process with a persistent multifractal information or news process. The infomation process is fractally clustered. This compounded multifractal diffusion model produces a multifractal interest rate process with a proper persistence level to match that of the empirically observed interest rate processes.

The fractal scaling property is one of the main key components that generate thick-tail and long-term dependence phenomena in time series, as explained by Mandelbrot (2001a, 2001b, 2001c, 2001d). Mandelbrot argues that both phenomena are common in nature (Mandelbrot, 1982). Moreover, the MMAR produces a martingale, or no-arbitrage, pricing process, in contrast to the monofractal fractional Brownian motion, which does not produce a martingale and allows for a limited form of arbitrage (Rogers, 1997).

Since the MMAR is partly based on the monofractal factional Brownian motion, identification of the global degree of persistence of the financial time series is required. Table 1 provides a summary of recent published measurements of such degrees of persistence of financial market time series. There are two salient observations in this Table. First, none of the published measurements include option markets. Second, many reports appeared only in 2004. This avalanche of recent publications suggests that the topic is rapidly gaining interest in the financial community, but also that there are still important gaps in the published empirical research.

[INSERT TABLE 1 ABOUT HERE]

Calvet and Fisher (2002) state that the MMAR is a hybrid between jump diffusion models and the GBM, such that the MMAR contains all necessary characteristics found in the observed empirical data. Table 2 adapted from Mandelbrot, Fisher, and Calvet (1997) and Calvet and Fisher (2002) suggests that the MMAR is superior to other time series models in the aspects needed for modeling financial time series. It produces a martingale process with time-frequency scaling and thus Long Memory.

[INSERT TABLE 2 ABOUT HERE]

Beside the MMAR, only the Fractional Integrated GARCH (or FIGARCH) and GARCH models can exhibit the empirically observed volatility clustering in return series, while preserving the desirable no-arbitrage martingale property or One-Price-Law. The monofractal FBM, ARFIMA, and ARMA models all exhibit correlation in the return series without this desirable martingale property. These non-martingale models all provide arbitrage opportunities and don't adhere to the no-arbitrage One-Price-Law. Also, the MMAR as a continuous time model has an advantage over its discrete model candidates, because it can be used with very high frequency (*e.g.*, tick-by-tick) data.

# 3 Interest Rate Data

The empirical U.S. Treasury interest rate series are obtained from the Federal Reserve Bank of St. Louis web site (H.15). This paper uses the daily computational interest rate series, called Treasury constant maturity, with 3-month, 6-month, 1-year, 2-year, 3-year, 5-year, 7-year, and 10-year maturities.[1] In addition, the Fed Funds rate, which is often used as an instantaneous rate for affine interest rate models, is also analyzed.

The interest series in this study cover the period of April 13, 1987 – December 31, 2002.

[1] In addition, the secondary market rates are analyzed, and the results suggest that these rates do not exhibit the long memory effect. The degrees of persistent $H$ are slightly below 0.5.

This approximate 15-year period provides 4096 daily observations. This length of the data set is necessarily chosen such that it is conform the processing capacity of a simple personal computer. Moreover, Los (2003) suggests business cycles last approximately 10 to 12 years. Thus, the 15-year period is expected to cover at least one whole business cycle in the USA. Each interest rate series for any maturity has the same number of observations. Like in McCarthy *et al.* (2004), missing values were replaced with the rate from the previous day. The same length of period is used to compute the partition function (sample sum), scaling function, Legendre multifractal spectrum, and homogeneous or monofractal Hurst exponent.

# 4 MMAR: Detection, Identification, Synthesis, and Simulation

The purpose of this paper is to identify the diffusion processes of the eight interest rate ("node") series of the U.S. Treasury term structure and their coherent system, as well as of the Fed Funds rate. Only the first five moments of the nine simulated interest rate paths are most thoroughly analyzed.

The Multifractal Model of Asset Returns (MMAR) was initially proposed by Calvet *et al.* (1997), Fisher *et al.* (1997), Mandelbrot *et al.* (1997), Calvet and Fisher (2002) and empirically tested with the foreign exchange rate, the U.S. stock index, and the individual U.S. stocks. In addition, Fillol (2003) has successfully applied the MMAR to the French Stock Index.

Unlike McCarthy *et al.* (2004) who use the Haar Wavelet to measure the degree of persistent or (Global) Hurst exponents of the Treasury rate series across the maturities, this paper examines the multifractal process of the Treasury rate series, identify the parameters of their corresponding MMARs, and compare the performance of these multifractal models with the respective GBM and GARCH(1, 1) processes.

The procedure of MMAR begins with identifying the multifractal spectra of the time series of interest rates, computing the values of their few particular parameters, synthesizing the mul-

tiplicative measure that preserve the multifractality properties, and simulating the compounded processes of the pricing GBMs driven by the multifractal trading time information processes.

The MMAR is a stochastic process $X(t)$, such that

$$X(t) = \ln P(t) - \ln P(0) \tag{1}$$

where $P(t)$; $0 \leqslant t \leqslant T$ is the price series while $t$ represents conventional clock time. Thus, $\{X(t)\}$ is a multifractal process that has the following properties:

Assumption 1: $X(t)$ is a compounded process, where a Brownian Motion operates on a multifractal trading time function:

$$X(t) \equiv B_H[\theta(t)] \tag{2}$$

where $B_H[.]$ is a fractional Brownian Motion (FBM) and $H$ is a Hurst exponent with $0 < H < 1$, with trading time $\theta(t)$. The $\theta(t)$ process deforms or "warps" the multifractal information process in conventional clock time into equally-distanced trading time, while the $B_H[.]$ process operates the interest rate pricing process.

Assumption 2: trading time $\theta(t)$ is the cumulative distribution function (c.d.f.) of a multifractal measure defined on the time axis $[0, T]$. It reflects the actual news dissemination process that affects the volume of trades on the trading floors. It changes the unequally-spaced, or clustered trading events, into equally-distanced fractal trading events, that form the multifractal information process that drives the GBM pricing process.

Assumption 3: the return generating pricing process $B_H[.]$ and the multifractal infomation process, or trading time function $\theta(t)$ operate independently of each other. In other words, although the interest rate markets are driven by the trading events, their pricing operation is mechanically independent of them.

The principle here is that one can transform a monoscaling process like the monofractal Brownian motion into a multiscaling process by properly mapping the one dimensional time domain $t \longrightarrow \theta(t)$ where the trading time possesses all the multifractal properties that are expected to

be passed on directly to the pricing FBM. The Hurst exponent of the second moment of the final interest rate process $B_H[.]$ is then about (but not quite!) the "average" of the (second moment) neutral Hurst exponent ($H = 0.5$) of the standard GBM and the persistent (second moment) Hurst exponent ($0.5 < H < 1$) of the information process. The model identification begins with determining the Hurst exponent of the interest rate process $B_H[.]$, from which the Hurst exponent of the information process or trading time $\theta(t)$ is then inferred, based on the fitted shape of the multifractal spectrum.

## 4.1 Identification of Scaling Properties and Multifractal Spectra

With the goal of tractability, the detection of the multifractality of the interest rates begins with the use of Gibbs' partition function

$$S_\delta(T,q) = \sum_{i=1}^{n} \left| X_{\lceil i\cdot\delta \rceil} - X_{\lceil (i-1)\cdot\delta \rceil} \right|^q \tag{3}$$

where $\lceil\cdot\rceil$ is the integer part operator, and $\delta$ is the time increment.

By the definition of multifractality, a stochastic process $X(t)$ is multifractal if it has stationary increments and satisfies the fractional moment relationship

$$E\{|X(t)|^q\} = c(q)t^{\tau(q)+1} \tag{4}$$

for all $t \in B, q \in Q$, where $E\{\cdot\}$ is the expectation operator and $c(q)$ is called a prefactor. $B$ and $Q$ are positive real numbers where $0 \in B$ and $[0,1] \subseteq Q$ . In other words, the movements of the process $X(t)$ are clearly scaled with the *scaling exponent* $\tau(q)$. The moments, $q$, can theoretically be negative. According to Mandelbrot *et al.* (1997) negative moments do not occur in financial data, but others (Los & Yalamova, 2003) found differently for some empirical stock market prices immediately after stock market crashes, when the "randomness" of the after-shock stock market pricing process is exceptionally high.

By logarithmic transformation, the partition function can be rewritten as

$$\log(S_\delta(T,q)) \approx \tau(q)\log(\delta) + \log[c(q)] + \log(T) \tag{5}$$

Clearly, this is a approximately linear relationship. This equation also implies that if any function has scaling properties, the logarithmic plot of the partition functions against the time increment should be approximately linear. With various moments, $q$, and incremental time, $\delta$, one can identify the scaling function, $\widehat{\tau}(q)$ , using various simple projection methods. Then, using the Legendre transform on the identified scaling function $\widehat{\tau}(q)$ one can identify the multifractal spectrum $\widehat{f}(\alpha)$ from this scaling function as

$$\widehat{f}(\alpha) = \min_{q}[q\alpha_L - \widehat{\tau}(q)] \tag{6}$$

where $\alpha_L$ is a localized Hurst exponent, or Lipschitz-$\alpha_L$.

## 4.2 Identified Hurst Exponents and Parameters of the Cascading Measures

Given that interest rate series shows such time-frequency scaling, Mandelbrot *et al.* (1997) and Fisher and Calvet (2002) have proven that the following identities hold.

$$\widehat{\tau}_X(\frac{1}{H}) = \tau_\theta(1) = 0 \tag{7}$$

$$\tau_X(q) = \tau_P(q) = \tau_\theta(Hq) \tag{8}$$

$$f_X(\alpha_L) = f_P(\alpha_L) = f_\theta(\frac{\alpha_L}{H}) \tag{9}$$

The first identity allows the identification of the Hurst exponent $\widehat{H}$ of the log price series. This identification can be done by finding the partition function plot at a particular moment $q$ that is approximately parallel to the horizontal axis. In other words, the partition function plot of a particular $q$ and $\delta$ that has a zero slope can be used to solve backward for the Hurst Exponent of the interest rate process $B_H[.]$.

The second identity suggests that the log price and price processes, $X(t)$ and $P(t)$, respectively, have the same scaling function, while the scaling function of the trading time has the same shape, but is shifted by the factor of $Hq$.

The third identity indicates that the multifractal spectra of the processes $X(t)$ and $P(t)$, each computed by using the Legendre transformation of the scaling function, are the same. Again, the

multifractal spectrum of the trading time has the same shape, but shifted by a factor of $\frac{\alpha_L}{H}$. This last identity is very important for constructing the MMAR and will be used in next section.

### 4.3 Synthesizing the Lognormal Measures

Multiplicatively cascading probability measures are a key for reconstructing the MMAR from the identified parameters. They have all ideal scaling properties that will be transferred to the simulated FBM, exhibiting the identified long-term dependence when the two processes are compounded. The cascading probability measures are normally used to generate positive multifractality using iteration techniques. The value of the multiplicative measure, $\mu_{k,b_k}$ built on a single mass $M_0^0$, after $k$ iterations at interval $B_k$, is given by

$$\mu_{k,b_k} = M_{b_k}^k \cdot M_{b_{k-1}}^{k-1} \cdots M_{b_1}^1 \cdot M_0^0 \tag{10}$$

for any dyadic (= by a factor of 2) partitioning of the intervals. The initial probability mass $M_0^0$ is "divided" up by multiplying by a cascade of probability measures to result in a final empirically realistic distributional measure $\mu_{k,b_k}$.

There are several extensions of these multiplicatively cascading probability measures. One can introduce stochastic probability measures by using any known distribution, *e.g.*, the Gaussian distribution. Empirically, one can ascertain, by examining their multifractal spectra, that most financial time series, including interest rates, exhibit multifractal spectra with humped shapes, while their trading time is the cumulative distribution function (c.d.f.) of multiplicative random probability measures with simple lognormal masses (c.f. Bailli *et al.,* 1996; Bollerslev, 1986; Calvet *et al.*, 1997; Calvet and Fisher, 2002; Mandelbrot *et al.*, 1997).

Calvet *et al.* (1997) proved that the multifractal spectrum function of trading time with lognormally distributed masses is

$$f_\theta(\alpha_L) = 1 - \frac{(\alpha_L - \lambda)^2}{4(\lambda - 1)} \tag{11}$$

where $f$ is hump-shaped and symmetric around its maximum or most probable Hurst exponent,

$\widehat{\alpha}_{L0} = \lambda$.[2] The first two moments of the lognormal distribution are as follows;

$$\widehat{\lambda} = \frac{\widehat{\alpha}_{L0}}{H}, \text{ and} \tag{12}$$

$$\widehat{\sigma}^2 = \frac{2(\widehat{\lambda} - 1)}{\log\ b} \tag{13}$$

where $b = 2$. This suggested closed form solution is very useful for the synthesis of the measure that leads to obtaining trading time in the MMAR.

With the identified mean and variance, the multiplicative lognormal probability measure path can be synthesized for a length of $2^K$, which should be greater than the desired length of simulated interest rate series. For each step of the construction of the multifractal lognormal probability measure path, we draw the masses $M$ where $-\log_b M \sim N(\widehat{\lambda}, \widehat{\sigma}^2)$.

According to the MMAR architecture, the key parameter is $\widehat{\lambda}$. There are two methods that can be used to identify $\widehat{\lambda}$. The first method uses the relation $\widehat{\lambda} = \frac{\widehat{\alpha}_{L0}}{H}$ and obtains the first moment $\widehat{\lambda}$ directly from the multifractal spectrum of the log price process $f_X(\alpha_L)$ (Fillol, 2003).

Calvet and Fisher (2002) propose a second method by fitting the $f_X(\alpha_L)$ for the $\widehat{\lambda}$. Let the most probable exponent $\alpha_{L0} = \lambda H$, then the log-price series $X(t)$ has the following quadratic multifractal spectrum

$$f_x(\alpha_L) = 1 - \frac{(\alpha_L - \alpha_{L0})^2}{4H(\alpha_{L0} - H)} \tag{14}$$

Thus, if the Hurst exponent $H$ is known, the only free parameter $\alpha_{L0}$ can be obtained by a simple nonlinear fitting process. The identified $\widehat{\alpha}_{L0}$ then leads to the calculation of $\widehat{\lambda}$ and $\widehat{\sigma}^2$ using the equation 12 and 13. After a proper synthesis of the multiplicative lognormal probability measure path, the next step is to compute the c.d.f. of the synthesized measures. The resulting time function is then called the trading time, $\theta(t)$.

## 4.4 Simulation of the MMAR

The simulation of the MMAR can be conducted by compounding an FBM with the corresponding trading time. Calvet and Fisher (2002) and Fillol (2003) obtain a simulated FBM by comput-

[2] See proof in Calvet *et al.* (1997)

ing the cumulative sum of the simulated fractional Gaussian Noise (FGN) with respect to the identified mono-fractal Hurst exponent $\widehat{H}$. The authors do not explicitly describe the particular simulation algorithm and interpolation of the FBM process and the MMAR used in their studies. Nevertheless, the overall scheme of the MMAR construction is as follow.

A finite-stage synthesis of a multifractal probability measure is obtained following the preceding section. The length of synthesized measure path must be corresponding with the desired length of the MMAR. For example, under the dyadic base of 2, if a simulated MMAR of length $T$ is required, the length of measures will have a minimum integer number of stages $k$ such that $2^k \geq T$. At each stage $k$, independent log-normal multipliers, or masses $M$, that have distribution with respective to those mean and variance obtained from the empirical series, are drawn. Once all $k$ stages are finished, the cumulative sum of the measures, a discrete approximation to the quadratic variation of a multifractal path, provides the accumulated trading time $\theta(t)$.

A discretized path of an FBM $B_H[.]$ in this study is generated by simulating the first differences of FBM $B_H(t) - B_H(t-1)$, which is called fractional Gaussian Noise (FGN) with parameter $H$. The covariance at lag $k$ of FGN follows:

$$\begin{aligned} \gamma(k) &= Cov[B_H(t) - B_H(t-1), B_H(t+k) - B_H(t+k-1)] && (15) \\ &= \frac{\sigma^2}{2}(|k+1|^{2H} - 2|k|^{2H} + |k-1|^{2H}), \text{ and} && (16) \end{aligned}$$

for $0.5 < H < 1$, the process is persistent, while for $0 < H < 0.5$, the process is anti-persistent. Thus, one can simulate either the FBM $B_H[.]$ directly, or the FGN and compute its cumulative sum to obtain the FBM. The simulated FBM then can be compounded with the trading time using any proper interpolation.

# 5 Empirical Results

Our empirical analysis begins with the plot of the US term structure across nine maturities. Figure 1 shows the time series plot of the eight Treasury rate and Fed Funds rate series altogether. This

plot suggests various shapes of the term structures over time. First, consider only the constant maturity rates. For most of the time period, the US Treasury term structure exhibits an upward-slope, where in the picture the band of the plots is wide. The slope of the term structure becomes less and possibly flattens out in the first quarter of years 1989, 1995, 1997, and 2000. The flat slope with a potential of humped shape of the term structure can be seen over the period between years 1989 and 1990.

[INSERT FIGURE 1 ABOUT HERE]

The Fed Funds rate behaves differently during the studied period. In late 1980s, the Fed Funds rate does not conform with the constant maturity term structure. During the period between 1987 and 1990 the Fed Funds rate, which is an overnight borrowing rate, is higher than the 3- and 6-month as well as 10-year constant maturity Treasury rates. However, after year 1990, the Fed Funds rate conforms more with the whole term structure. The plot reflects these discernible interventions by the Federal Reserve in the Fed Funds market. In addition, the Fed Funds plot contains more spikes and jumps than the Treasury rates do. This may be because financial institutions like commercial banks have to determine their reserves at the end of the two-week reserve settlement periods. They can end up with very high interest rate borrowing transactions in order to meet the legal bank reserve requirements by their bi-weekly deadlines.

Figure 2 plots the logarithmic first difference of all nine return series with their identified monofractal price and trading time Hurst exponents. Since the Hurst exponent is a measure of persistence (where the higher the Hurst exponent, the more persistent the interest rate series), the fact that the short-rate series are more persistent ($H > 0.5$) than the long-rate is ($H = 0.5$) is one of our unexpected findings. But notice that the Fed Funds rate that has an anti-persistent $H = 0.48 < 0.5$. Our explanation for this anti-persistence, or fast mean-reversion, is that the Fed Funds rate is an overnight rate on irregular interbank bank repurchase agreements, which are reversed within the time unit of this paper, which is one day (= 24 hours).

[INSERT FIGURE 2 ABOUT HERE]

The 10-year maturity Treasury rate series explicitly shows the neutral mean reversion over the studied period and hardly indicates any singularities (or jumps). Apparently, this behavior is similar to that of a standard GBM and is supported by the calculated Hurst exponent of 0.5. Moving to the shorter maturity rates of return, the Hurst exponent monotonically increases from 0.5 to 0.57, except the jump of Hurst exponent at the 6-month return series to $H = 0.59$. Moreover, the plots themselves reveal a very stunning picture of the singularities or jumps and heteroskedastic volatility clustering (= "intermittency") in short maturity Treasury interest rate series, *e.g.*, the time series plot of the 3-month and Fed Funds return series.

A possible behavioral explanation for the observed persistence of most of the interest rates, in particular at the short term end, may be that the Federal Reserve auctions the Treasury papers in auctions with about 40 primary dealers. In contrast, the Fed Funds market is an open market with hundreds of commercial banks.

## 5.1 Time-Scale Analyses of Empirical Treasury Rates

The time-scale analysis begins with the longest maturity Treasury rate series. Figure 3 provides the analytical profile of the 10-year Treasury rates including in panel a) the rebased partition function $S_q(T, \delta)$; in panel b) the scaling function $\tau(q)$, in panel c) the multifractal spectrum $f(\alpha_L)$; and in panel d) the quadratic fitting of the multifractal spectrum. Panel (a) in figure 3 exhibits the partition functions, $S_q(T, \delta)$, plotted against the base-2 logarithm of investment horizon, $\log_2 \delta$, covering the first five integer moments of the distributions including the zeroth moment. This time-scale analysis allows an investigation of fractional moments. However, this paper focuses on the first few integer moments common in the financial literature. The plot starts from the zeroth moment $q = 0$ (the lowest line) with a unit increment and ends at the fifth moment $q = 5$ (the highest line). The nearly straight plot suggests that a particular scaling of moments exists and can be identified.

[INSERT FIGURE 3 ABOUT HERE]

Notice that the partition functions of the first three moments are nearly straight with some increasing variation when the investment horizon ($\delta$) becomes longer. The increasing variation of the higher order moments can affect the accuracy of the analysis and the MMAR parameters. It also suggests that the moment range of the scaling is limited. To sustain the accuracy this study uses the $2^6 = 64$ business days or the investment horizon of one quarter to obtain the MMAR parameters for all nodal market maturities unless otherwise stated.

Panel (b) provides the scaling function $\tau(q)$ plotted against the first five moments, $q = 1, 2, 3, 4$ and 5. The scaling function is obtained from the slopes of the partition functions in panel (a). The 10-year series scaling function is concave upward. It deviates from the straight line with the neutral $H = 0.5$ slope, which is the neutral scaling function slope of the GBM. By definition, the value of the scaling function is always equal to $-1$ at the zeroth moment. Evidently, when the moments are less than 2, the scaling function of the 10-year rate is slightly higher than that of the GBM. When the moments are greater, the scaling function becomes somewhat lower than that of the GBM. The neutral Hurst exponent of 0.5 the GBM is directly obtained from the scaling function using the relationship shown in the previous section, indicating the near GBM of the 10-year series. But the slight concavity of the 10-year scaling function $\tau(q)$ shows that there exists even a bit multifractality in the 10-year interest rate series.

As shown, panel (c) indicates the quadratic-like multifractal spectrum, $f(\alpha_L)$, of the 10-year rate series obtained from Legendre transformation of its scaling function. The multifractal spectrum is simply the entire distribution of the Hurst exponents of the series with a humped shape and maximum of unity by default. A complete, parabola-like multifractal spectrum containing negative slopes can be obtained using a different method (Los, 2003).

Since the quadratic multifractal spectrum of the Treasury rate also implies the quadratic multifractal spectrum of its trading time, panel (d) assures us that the multifractal spectrum

$f(\alpha_L)$ of the 10-year Treasury rate is almost perfectly quadratic. The fitted line lies almost exactly on top of the empirical multifractal spectrum, but slightly deviates when the Hurst exponents are less than 0.4. Using the multifractal spectrum of the rate series and the closed form solution of the lognormally distributed multifractal spectrum of trading time in the preceding section, the most probable Hurst exponent of its trading time is calculated to be $\alpha_{L0} = 0.56$, which helps to identify the first two moments of lognormally distributed measures, which are $\widehat{\lambda} = 1.11$ and $\widehat{\sigma} = 0.22$, respectively. These two moments will be used later in the synthesis of measures and simulation of the MMARs. Notice that the trading time shows more persistence than the Brownian motion of the interest rates, since that has a neutral Hurst exponent of $H = 0.5$.

The results of other maturity Treasury term structure rates are quite similar. The only differences include the greater increasing variation found in the partition functions and the larger deviations between the fitting and empirical multifractal spectra. Somewhat to our surprise, the Fed Funds rate series show partition functions over a very limited range of moments, suggesting that it hardly scales, with some globally identifiable anti-persistence ($H < 0.5$). In other words, the Fed Funds market is highly idiosyncratic (or chaotic?), due to its ever-changing absolute reserve requirements (which are volume constraints and not price constraints), and it does not allow for much distributional consistency over time.

Table 3 provides all necessary MMAR parameters for each maturity. This is the collection of the time series models for each of the nine nodal interest rates in its simplest parametrization. Being able to handle the heteroskedasticity of the time series and preserving the correct scaling properties of the empirical data, the MMAR requires only four unambiguously identifiable parameters: the Hurst exponent $H$ of the interest ate process, the most probable Hurst exponent of trading time $\alpha_{L0}$, and the first two moments $\widehat{\lambda}$ and $\widehat{\sigma}^2$ of the lognormal distribution of the multiplicative probability measures. The list of MMAR's parameters begins from those series with the longest maturity, 10-year, to the shortest maturity, Fed Funds rate.

[INSERT TABLE 3 ABOUT HERE]

The persistence of interest rates is attributed to the highly persistent Hurst exponents $\alpha_{L0}$ of the multifractal trading time, *i.e.*, the exogenous news information process. In other words, while the theoretical pricing process may be a theoretical, neutral GBM, the empirically observed persistence of the process is caused by the clustering of the actual trading events, which is induced by the exogenous clustering of news events (Mandelbrot & Hudson, 2004).

The 10-year rate has the lowest $\alpha_{L0} = 0.56$ while the 6-month rate shows the highest value of 0.67. The value decreases slightly to 0.66 for the 3-month series and dramatically drops to 0.57 for the Fed Funds rate. One wonders if this phenomenon is related to the frequency of the respective Treasury auctions, or to the number of trading participants, or both. We know that a degree of persistence in a system process, like the beat of a healthy human heart, is determined by the degrees of freedom of the trading process, but we still don't know how these two are precisely related. This is an important potential market micro-structure research problem, ideal for another PhD candidate.

The first moments of the lognormally distributed measures $\widehat{\lambda}$ do not show any systematic characteristic. Evidently $\widehat{\lambda}$'s across maturities are larger than one, since the series of trading events show more clustering than the actual interest rate pricing. The maximum of the $\widehat{\lambda}$'s is 1.183, which is for the Fed Funs rate series, suggesting that the Fed Funds market has the most tenuous relationship between the degree of persistence of its market and the degree of persistence of its information process.

Interestingly, the variances $\widehat{\sigma}^2$ of those log normal probability measures seem to indicate a possible system for the multifractal spectra. The shorter maturity Treasury rates show a more dispersion of their multifractal spectra than those of interest rates with the longer maturities. This suggests that the shorter maturity markets are impacted by a wider variety of news events (including "rumors") than the longer maturity markets, which are dominated by the analytic

portfolio management of long term institutional investors.

Overall, all studied interest rate series show Long Memory, except the 10-year rate, which is very close to the neutral memory of the GBM, and the Fed Funds rate, which is anti-persistent and has a "negative memory." Moreover, the results indicate the non-Gaussian distribution, the existence of higher moments, nonlinearity, and time-and-frequency scaling properties in the Treasury series. These findings provide rather conclusive empirical evidence against the popular GBM driven low-factor models in the current term structure literature, which assume a neutral Hurst exponent $H = 0.5$. As a part of MMAR's performance measurement relatively to those of GBM and GARCH(1, 1) processes, the parameters of the GARCH(1, 1) models for all studied Treasury rate and the Fed Funds rate series are collected in Table 4, while those of the GBM simply are the first two moments of the studied return series.

[INSERT TABLE 4 ABOUT HERE]

## 5.2 Comparative Analysis of Simulated Results

First, the performance of MMAR is tested by investigating how effectively it can preserve the Long Memory found in the empirical series. The monofractal Hurst exponent for each simulated MMAR is identified for each maturity. The resulting Hurst exponents are then averaged for each maturity and then reported in Table 5.

[INSERT TABLE 5 ABOUT HERE]

As expected, the average Hurst exponents for all Treasury maturities are identical to those Hurst exponents fed into the simulation algorithm, except the 10-year rate, where the average Hurst exponent is 0.4% larger than the corresponding input. Notice that the average of the simulated MMARs of the Fed Funds rate has a quite different degree of anti-persistence than found in the empirical series. It is very difficult to comparatively simulate anti-persistent series than persistent series, because the anti-persistent series mean-reverts within the observational time

unit of one day. In short, these results provide numerical support that the MMAR can effectively preserve the monofractal Hurst exponent for studied Treasury rate series across maturities. But, like the GBM and the GARCH(1, 1) models the MMAR has difficulty with the simulation of the anti-persistent and highly idiosyncratic Fed Funds series.

Table 6 presents the identified scaling exponents or slopes of the partition functions for the first five integer moments of the empirical Treasury rates and the mean scaling exponents of those simulated MMAR, GBM, and GARCH(1, 1) series with the maturities longer than two years. Tables 7 and 8 present the scaling exponents for those Treasury series with the maturities less than three years and the Fed Funds rate series, respectively. The mean scaling exponent of the simulated series is calculated by averaging those scaling exponents of the $1,000$ simulated series for each process. The mean scaling exponents of the simulated GBM series for all maturities are almost exactly the same. Their scaling exponents increase approximately by 0.5 for each moment order $q$. Although the results are not surprising, they ensure that the scaling analysis and simulation methods in this study are reliable and mutually compatible. In addition, the scaling functions of the simulated GBM for the studied maturities obviously deviate from those of empirical Treasury rate series.

[INSERT TABLE 6 ABOUT HERE]

[INSERT TABLE 7 ABOUT HERE]

[INSERT TABLE 8 ABOUT HERE]

Moving to the simulated GARCH(1, 1), their scaling exponents for the first two moments are almost constantly at $-0.5$ and 0, respectively. The scaling exponents of higher moments show some minor deviations from those of simulated GBM series as well as from those of the empirical series. In fact, the average of the identified slopes of the simulated GARCH(1, 1) series seems to follow those of the GBM for all studied moments. Thus, the results again suggest that the GARCH(1, 1) model does not properly identify the empirical Treasury rate processes. In particular, the scaling

exponents of the fourth and fifth moments are higher than those of the empirical interest rate series for most maturities.

Only the mean scaling exponents of the simulated MMAR represent the scaling exponents of empirical series well. The MMARs preserve the scaling properties accurately for the low moments across maturities, while the mean scaling exponents of the fourth and fifth exponents are lower than those of empirical series across maturities, except in the case of the exceptional Fed Funds rate. Remarkably, the mean scaling exponents of the simulated MMARs almost perfectly match those of empirical series for 1-year, 2-year, and 3-month maturity rates. More interestingly, the mean estimated slopes of MMARs for the second moment across all studied maturities are very accurate and far superior to those of simulated GBM and GARCH(1, 1), except for the Fed Funds series where the mean estimated slope of GBM is closer to that of the empirical series. Both simulated GBM and GARCH(1, 1) processes can closely preserve only the estimated slope of second moment for the 10-year maturity only.

In Tables 6, 7, and 8 the minimum and maximum of the $1,000$ simulated scaling exponents for each process across maturities are reported in parentheses. Another measure of performance is to measure the range (maximum - minimum) of the simulated scaling exponents. All simulated processes show that their ranges grow very slowly from the first to fifth moments, and similar results appear across all maturities, except for the Fed Funds rate where the range is significantly wider.

For the first moment, the uncertainty ranges of the GBM and GARCH(1, 1) are very similar. However, on average the ranges become wider for higher moments relative to those of the simulated GBM series. The range of the GARCH(1, 1) process seems to expand when the maturities become shorter. Although having a narrow range of uncertainty over the five moments, both simulated GBM and GARCH(1, 1) series do not exhibit correctly identified slopes of partition functions found from the empirical series for most of maturities. Unlike the GBM and GARCH(1, 1), the MMAR converges on average to the correct scaling functions, although it exhibits wider uncertainty ranges.

The difference between uncertainty ranges among the three processes are more pronounced for the third to the fifth moments in which these ranges expand more quickly, particularly when the moments increase. Also, the ranges of the simulated GARCH(1, 1) series seem to expand rapidly and become close to those of the MMARs when the maturities become shorter. An exception occurs in the case of the Fed Funds rate, where the uncertainty range of the GARCH(1, 1) for the higher moments is very close to that of the MMAR. This casts also doubt on the performance of the GARCH(1, 1) model as a correct model for the Fed Funds rate.

Although the deficiency of the MMARs relative to the other two processes appears to be their wider uncertainty ranges of its simulated scaling exponents, their averages of identified slopes for each moment are very accurate relative to the empirical series.

## 5.3 Snapshot vs. Time-Frequency Distributions

In this section, the best candidate of $1,000$ simulated series from each process is identified using wavelet multiresolution analysis (MRA). The performance measurement of the MMAR and comparative models begins with the investigation of how effectively the models preserve the entire time-frequency distribution found in the empirical series.

### 5.3.1 Frequency Distributions

Figure 4 provides the snapshot distribution comparisons between those of the empirical Treasury rate series with maturities longer than 2 years and their corresponding simulated series.

[INSERT FIGURE 4 ABOUT HERE]

As seen from panel a, the solid line exhibits the wavelet compiled density function (distribution) of the 10-year Treasury return series. With a high peak around mean, thick tails, and a small hump at each side of the tails, the empirical distribution clearly deviates from the Gaussian distribution shown by the dotted-dashed line, while the dashed line shows the compiled distribution of the corresponding simulated GARCH(1, 1) series. Although very similar to each other, neither the

simulated GBM nor the GARCH(1, 1) distribution is similarly shaped as the empirical distribution. Only the dotted line indicating the compiled distribution of the simulated MMAR has a shape that is similar to that of the empirical distribution. But the peak of the simulated MMAR distribution is still too high. The MMAR does get the kurtosis around the central tendency correct, but deviates from the empirical in the moderate tails.

Panels b, c, and d provide the comparisons of those compiled densities with the density of the 7−, 5−, and 3−year maturities. The overall result is similar to that of the 10-year maturity series. Only the simulated MMAR distribution can replicate the shape of the empirical distribution, while the distributions of the GBM and GARCH(1, 1) are very close to each other (= Gaussian distribution, unsurprisingly, since both are linear models of Gaussian distributions).

Figures 5 shows the comparison of the compiled distributions for the Fed Funds rate and its corresponding simulated series. Although the identification of the MMAR of the Fed Funds series faces some difficulties, its compiled distribution of the MMAR is very similar to the empirical distribution and clearly superior to those of the GBM and GARCH(1, 1).

[INSERT FIGURE 5 ABOUT HERE]

The figures suggest that the peakedness of the empirical distributions seems to be slightly higher when the maturities become longer. Also, the dispersion width is less when the maturities increase. Moreover, the plots make the scaling distribution preservation of MMARs more visible. Nevertheless, these plots are only a snapshot of the time-varying distributions. Wavelet MRA is used to thoroughly investigate the MMAR's performance overtime and scale.

### 5.3.2 Scalograms: Time-Scale (Frequency) Distributions

The continuous wavelet MRA of the interest rate series results in a scalogram that is a graph with time on the horizontal axis and different scales (= inverses of frequencies) on the vertical axis. It traces the second moment, variance, or energy of the interest rate series over a certain time period of $4,096$ days and over scales $1 - 64$ except the scales of the Fed Funds that range

from $1 - 256$. The absolute values or magnitudes of the localized wavelet resonance coefficients, generated by the wavelet transform at a certain scale and at a given time, are represented by color corresponding to the 128-color bar ranging from red (smallest variance) to blue and pink (largest variance). Analogously to the coefficients of determination $R^2$ of bivariate regression projections, the reddish-pink color on the scalogram indicates the highest correlation between the mother wavelet and the interest rate series at a particular time and scale.

Figure 6 provides the scalogram profiles for those empirical and simulated series with the 3-month maturities. The top left scalogram shows the localized variance of the empirical series at particular time moment on certain scales (or investment horizons). The top right scalogram plot belongs to the simulated GBM series. The lower right plot provides the scalogram of the simulated GARCH(1, 1) series, while the lower left scalogram plot shows the local variance analysis of the simulated MMAR. The scalogram of the simulated GBM series is clearly white noise. The scalogram of the GARCH(1, 1) shows some similarity to that of the empirical series. Nevertheless, the scalogram of the MMAR indicates its superiority over both the GBM and GARCH(1, 1) in being able to replicate the scaling properties of the empirical series.

[INSERT FIGURE 6 ABOUT HERE]

Examining other maturities of the Treasury rate series, the scalograms of the simulated GBM series are still white noise. The differences are obvious for the scalograms of the empirical series, where the red area appears more often over a time period relative to the longer maturity Treasury return series. The shorter the maturities, the more red areas appear on the scalograms. In addition, when the maturities become shorter, the magnitudes of the wavelet resonance coefficients seem to be smaller on average at all scales and at all times.

The scalograms of simulated GARCH(1, 1) indicate improvement, as more intermittent red areas begin to appear when the maturities are shorter. However, the color of the wavelet resonance coefficients is still different and indicates larger magnitudes than those of their corresponding

empirical series. As expected, the scalogram of simulated MMAR shows superiority over those of the simulated GBM and GARCH(1, 1) models by having a similar pattern of colors and clusters found in the empirical return series for these maturities. Nevertheless, the simulated MMAR scalograms still show too many yellow breaks at all times.

The scalogram analysis of the Fed Funds rate is shown in figure 7. The Fed Funds return series behaves very differently from the constant maturity Treasury return series in the preceding time-scale analysis and identification of the corresponding MMAR. The plot hardly indicates any clear singularities except some yellow background at the high scales, while the wavelet resonance coefficients seem to be very small as shown by the large red areas.

[INSERT FIGURE 7 ABOUT HERE]

But the Fed Funds rate is clearly not white noise. The empirical scalogram suggests even some periodicity and cyclicity. The horizontal line at the scale $a = 207$ over the period of $500-2,900$ days suggests a periodicity (= spectral line), while the horizon dashed line at the scale $a = 170$ running almost across the entire time period indicates a cyclicity (= periodically interrupted spectral line). Such cyclicity is usually an indication of chaos (= multiple coexisting price equilibria), in particular when combined with some periodicity. The Fed Funds market may periodically (bi-weekly?) cycle through a whole set of coexisting price equilibria.

Unlike the scalograms of the Treasury return series, where the simulated MMAR is always superior to the GBM and GARCH(1, 1), the scalogram of the Fed Funds rates appears different. In this exceptional case, the scalogram of the simulated MMAR no longer replicates that of the empirical series. Its background suggests too large magnitudes of the wavelet resonance coefficients. In contrast, the simulated GARCH(1, 1) scalogram seems to provide a better pattern of colors and, on average, has smaller wavelet resonance coefficients than the scalogram of the MMAR. This result might be attributed to an inaccurate identification of the MMAR in the preceding analysis due to the "randomness" of Gibbs' partition function at almost all moment

orders, while it exhibits some global anti-persistence.

Our modeling approach has one major drawback: theoretically, there should be a coherent forward relationship among all Treasury term structure nodes, as prescribed by the rational expectations theory, but this forward relationship is not explicitly modeled in the case of our 9-factor MMAR system. By construction, the MMARs are not designed to capture and reserve any multivariate interaction.

The top panel in Figure 8 presents the empirical term structure over the studied time period. One of $1,000$ simulated series for each maturity is selected and plotted in the bottom panel. It is clear that the design of the current term structure as a system of univariate MMARs does not provide the needed coherent relationship among the nodal maturities. The resulting term "structure" lacks the empirically observed coherence of Figure 1. Thus it appears that still better modeling of the nonlinear interaction between the nodal maturity markets is required.

[INSERT FIGURE 8 ABOUT HERE]

# 6 Conclusions

Treasury rates are the basis default risk-free rates in finance. A change in the levels and volatilities of these interest rates has a substantial impact on rational financial decision-making. Many theories have been proposed to explain the changes of level and the volatility of the term structure. Asset pricing modelers attempt to identify price diffusion processes from empirical financial market data. In particular, the Geometric Brownian Motion and the GARCH models are currently popular in these efforts.

This paper identifies Multifractal Models of Asset Return (MMARs) - recently introduced in the finance literature by Mandelbrot *et al.* (1997) - from the eight nodal maturities of the US Treasury rates and from the Fed Funds rate. The study shows that the Treasury rate and the Fed Funds series can be uniquely identified as multifractal Brownian motions. This study also improves the current MMARs with better numerical methodologies for the corroboration of the

identified Hurst exponents by wavelet multiresolution analysis.

After analytical, numerical, and graphical analyses of the Treasury rate series, the corresponding MMARs are synthesized and simulated with the exact Monte Carlo method, following the advice of Los (2003), who requires that every identified model be simulated to ensure that it can replicate the empirical features of the empirical data. The model performance results of these Monte Carlo simulations are then compared with not only the original empirical time series, but also with the simulated results from the corresponding GBM and GARCH(1, 1) processes. Moreover, this study visualizes, analyzes and compares the simulated results using wavelet scalograms, which allow the corroboration to be simultaneously conducted over time and frequency.

All eight maturity Treasury rates and Fed Funds rate series are identified as multifractal processes. The measures of their degree of persistence suggests that all eight Treasury rate series are persistent with respect to their time to maturity, while the Fed Funds rate series is globally mildly anti-persistent (It is also highly idiosyncratic and, probably, chaotic). It was surprising to find that, on average, the longer its maturity, the less persistent an interest rate process is.

Most of the time, the simulated MMARs outperform the corresponding identified and simulated GBM and GARCH(1, 1) models. The MMARs are clearly superior in preserving the distributional scaling of the empirical data. In addition, the simulated MMARs can closely trace the volatility of the empirical Treasury series for all eight maturities.

However, the MMAR, by default, cannot represent a complete model for the term structure. It fails to provide coherence to the dynamic term structure system among the nine maturities. Since there is considerable evidence suggesting that the term structure forms a coherent system, a multivariate system MMAR is needed for testing Los' (2003) cash flow theory of the term structure of interest rates. As of now, the univariate MMAR can only be an advanced model of the Market Segmentation Theory of the term structure of interest rates.

# 7 Figures

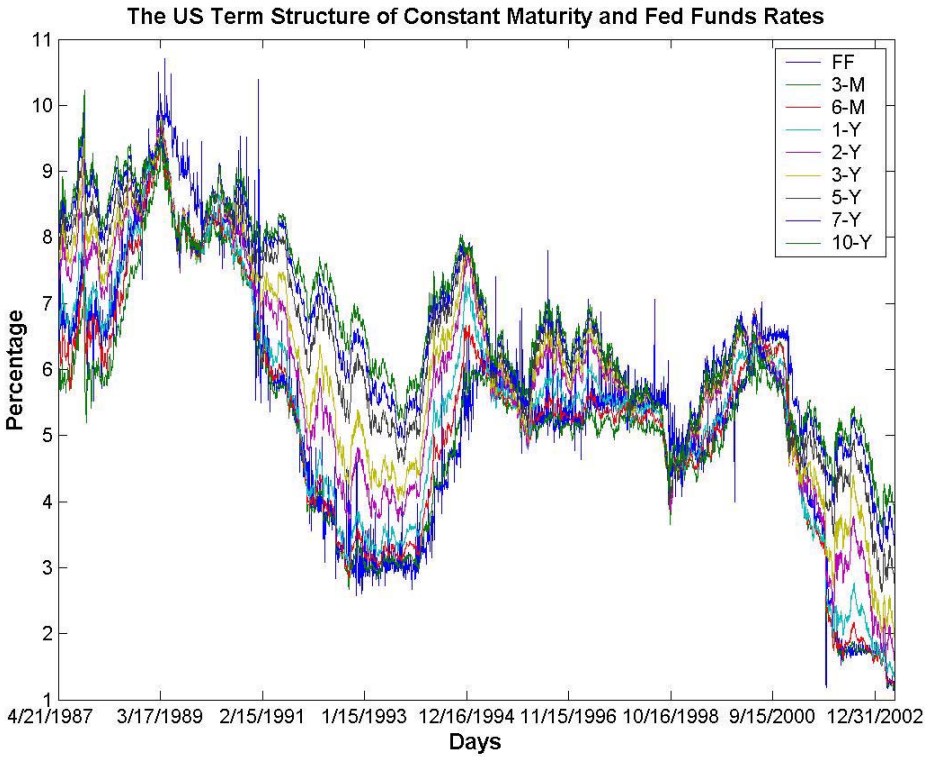


Figure 1: The Term Structure of Constant Maturity US Treasury and Fed Funds Rates. The US Treasury rates for eight maturities and the Fed Funds rate are plotted over time beginning from April 21, 1987 to December 31, 2002. For example, when the 10-year line is above the 3-month line, the term structure is upward-sloping. Vice versa, it is downward sloping. FF stands for Fed Funds.

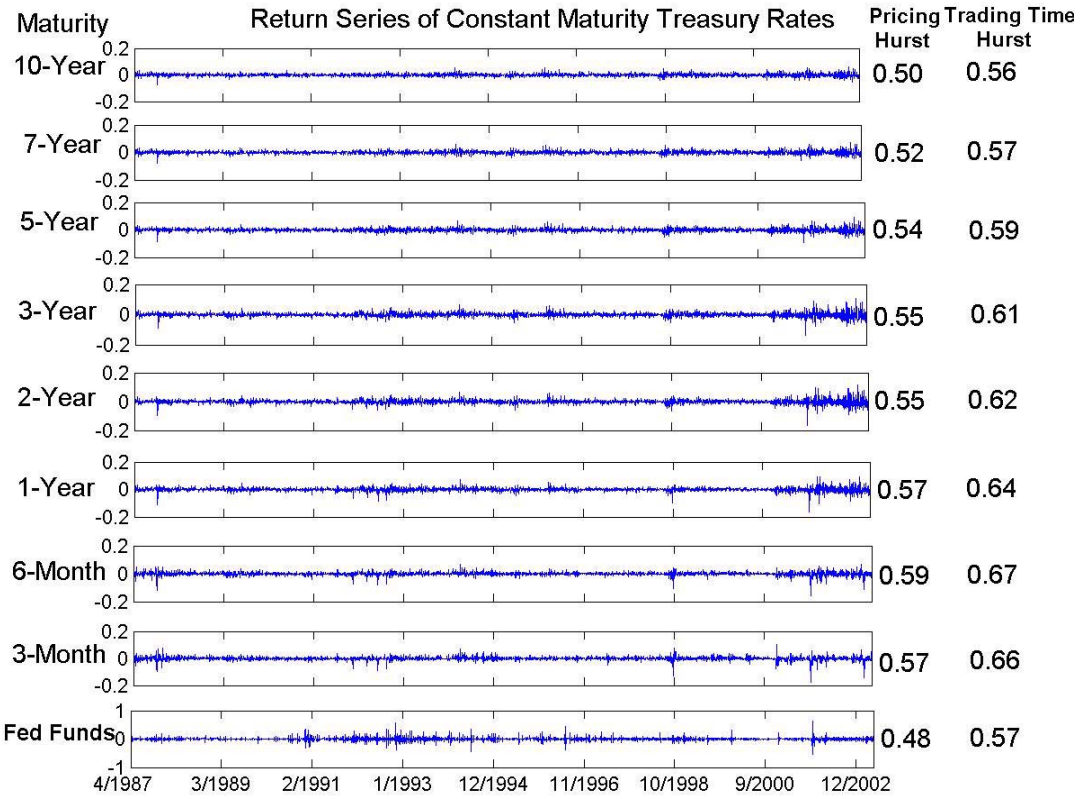


Figure 2: The Time Series Plot of Individual Return Series of the US Treasury and Fed Funds Rates (First Differences of the Logarithm of the Original Series). The left column indicates the maturity for each plot starting from the longest, 10-year maturity, to the shortest, Fed Funds, rates. The right two column next to the plots provides the degree of persistence or monofractal Hölder-Hurst Exponent identified by the Power Spectrum (Slope of Power Spectrum) method for each return series across studied maturities and its corresponding trading time, respectively.

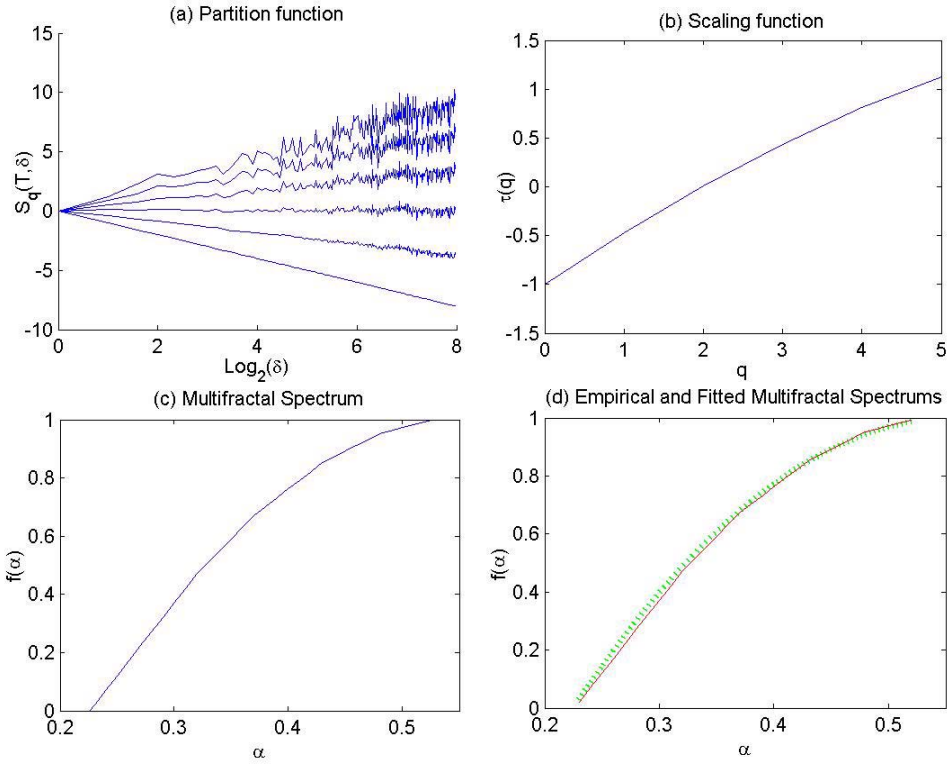


Figure 3: The Time-Scale Analytical Profile of 10-Year US Treasury Rate: April 1987 - December 2002. Panel (a) shows the partition function plots for the first five integer moments including zero. The function intercepts are normalized for comparison purpose. The highest line is for the fifth moment while the lowest line is for the zeroth moment. Panel (b) shows the scaling function plot of the Treasury rate across the five moments. Panel (c) provides the Multifractal Spectrum obtained from the Legendre Transformation of the Scaling function. Panel (d) shows that the Multifractal spectrum can be fitted by the quadratic function that leads to the detection of the MMAR's parameters.

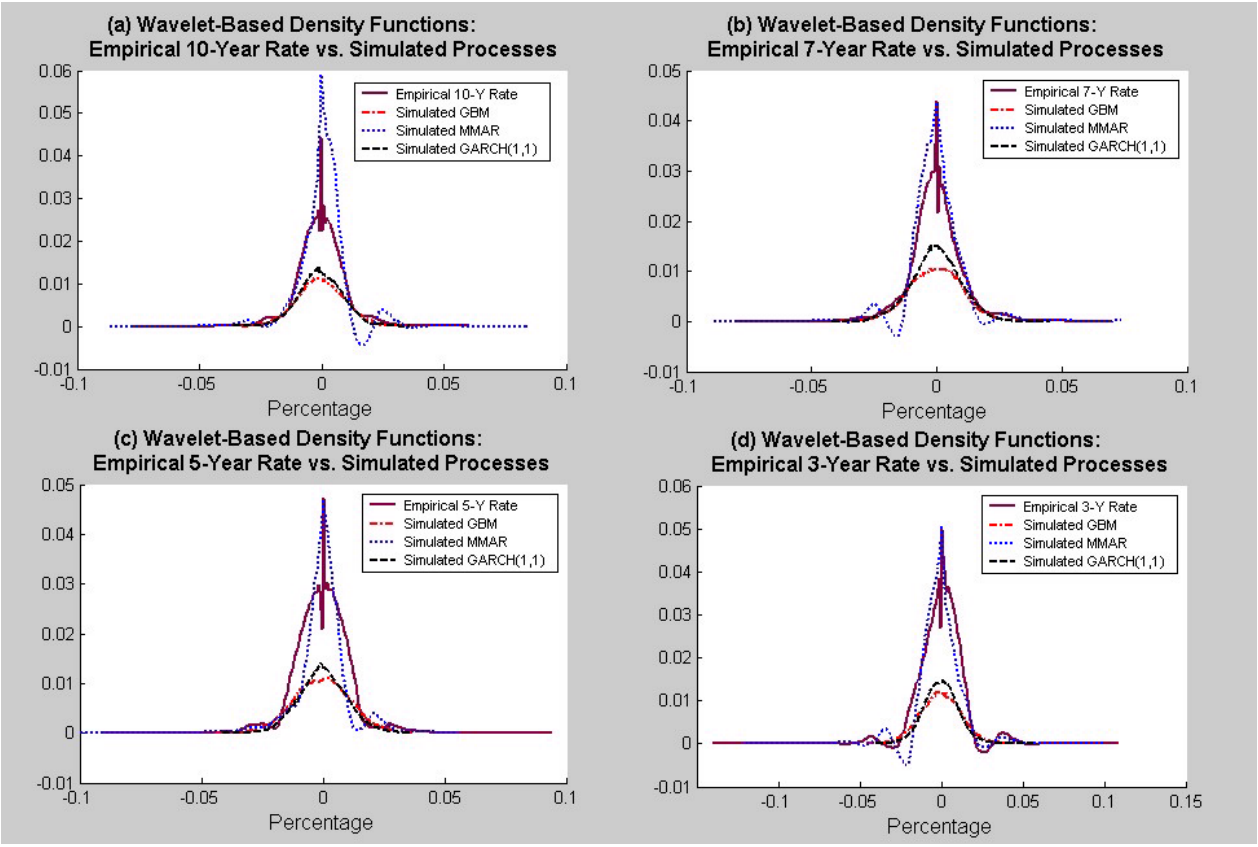


Figure 4: The Comparison of the Density Functions Identified by the Wavelet Transformation. The solid line indicates the density function of the empirical series. The dashed-dotted line indicates the density function of the simulated GBM. The dotted line indicates the density function of the simulated MMAR. The dashed line indicates the density function of the simulated GARCH (1, 1). Panel (a) shows the comparison of the densities for those series with 10-Year maturity. Panel (b) shows the comparison of the densities for those series with 7-Year maturity. Panel (c) shows the comparison of those densities from those series with 5-Year maturity. Panel (d) shows the comparison of those densities from those series with 3-Year maturity.

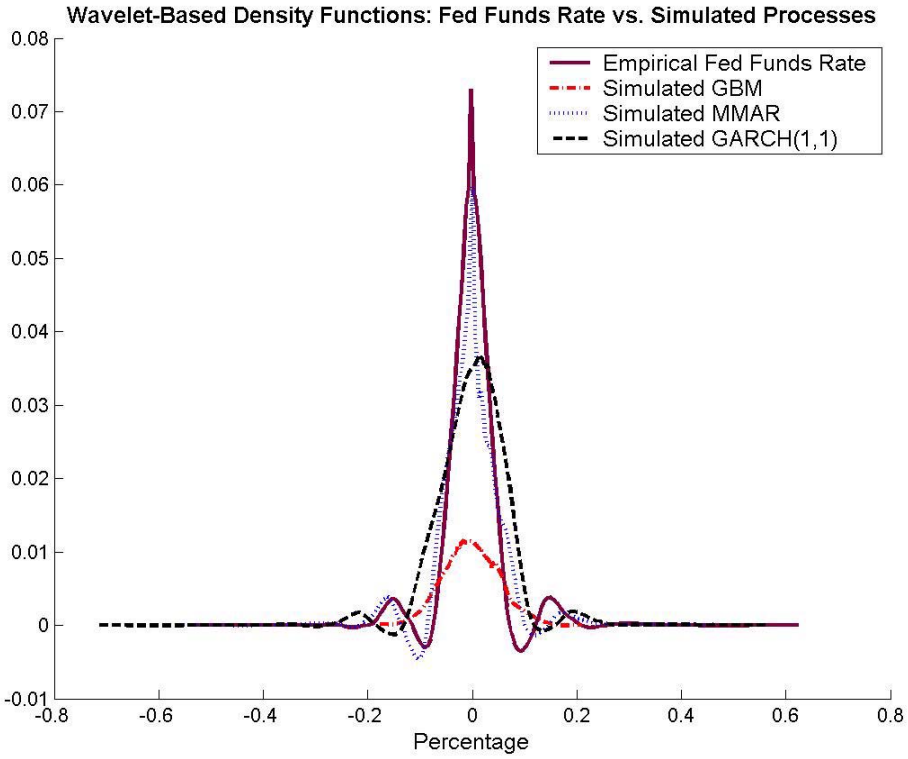


Figure 5: The Comparison of the Density Functions Identified by the Wavelet Transformation. The solid line indicates the density function of the empirical series. The dashed-dotted line indicates the density function of the simulated GBM. The dotted line indicates the density function of the simulated MMAR. The dashed line indicates the density function of the simulated GARCH (1,1).

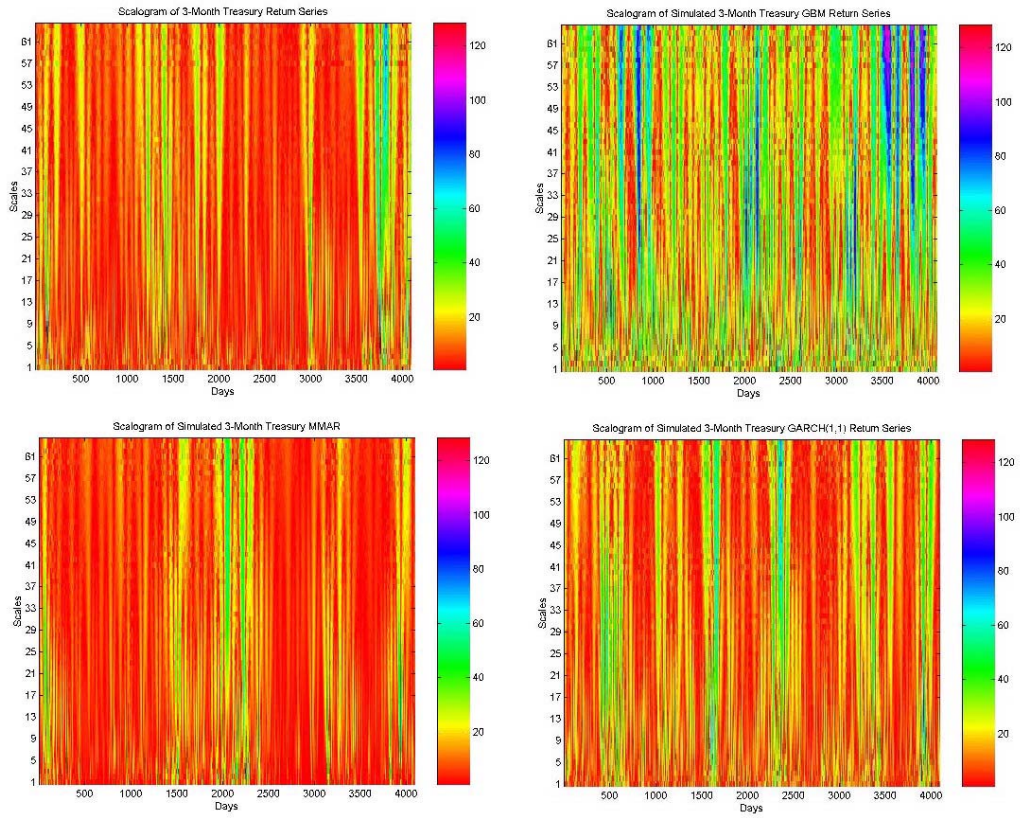


Figure 6: Scalograms of the 3-Month Treasury Return Series and Its Corresponding Simulated Processes. The upper left plot shows the scalogram of the empirical rate over the 4,096-day period and across the 1-64 scales. The magnitude of wavelet coefficients are colorized with a 128-color scheme. The wavelet used in the transformation process is the Morlet(6). The upper right scalogram is calculated from the simulated GBM having the empirical mean and variance. The lower right plot shows the scalogram of the simulated GARCH(1,1) return series while the lower left plot shows the scalogram of the simulated MMAR series.

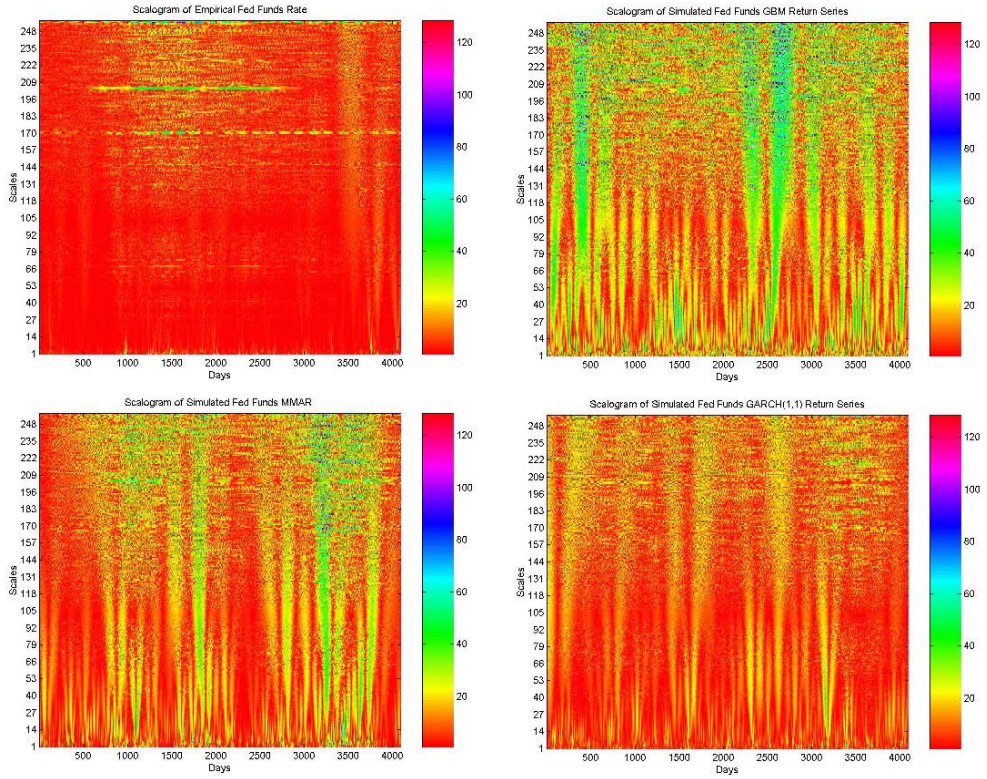


Figure 7: Scalograms of the Fed Funds Return Series and Its Corresponding Simulated Processes. The upper left plot shows the scalogram of the empirical rate over the 4,096-day period and across the 1-64 scales. The magnitude of wavelet coefficients are colorized with a 128-color scheme. The wavelet used in the transformation process is the Morlet(6). The upper right scalogram is calculated from the simulated GBM having the empirical mean and variance. The lower right plot shows the scalogram of the simulated GARCH(1,1) return series while the lower left plot shows the scalogram of the simulated MMAR series.

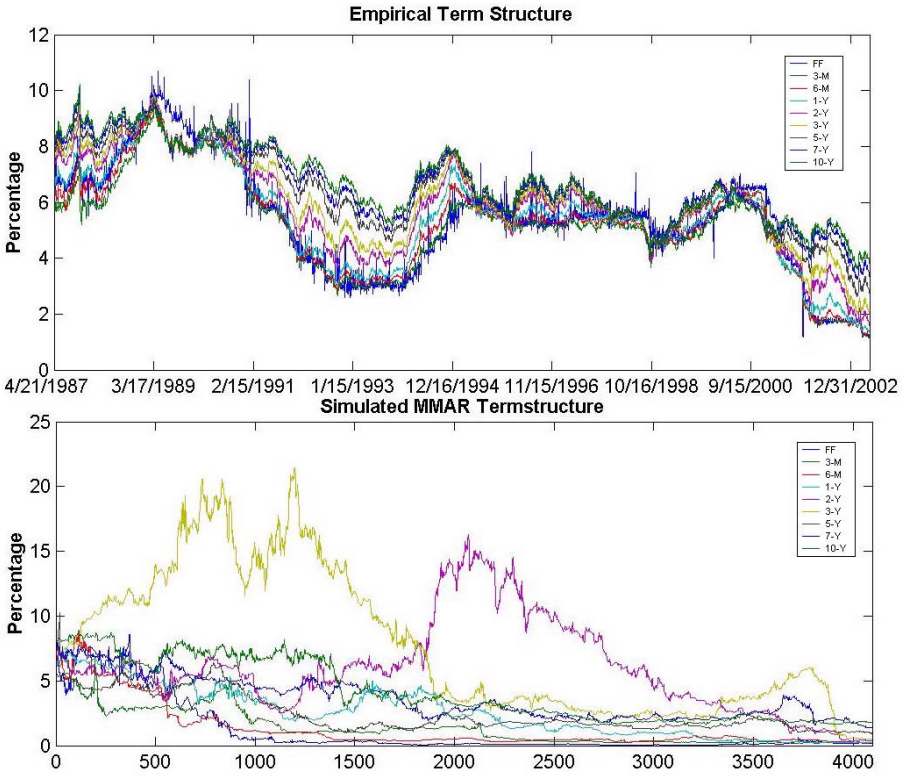


Figure 8: The Resulting Term Structure of Simulated MMAR. These graphs compare the empirical term structure with a simulated MMAR term structure.

| Author | Year | Hurst Exponents | | | | |
|---|---|---|---|---|---|---|
| | | Stock | Term Structure | Futures | Cash | Forex |
| **Karuppiah & Los** | **2005** | | | | | X |
| **Gil-Alana** | **2004** | | | | X | |
| **Lillo & Farmer** | **2004** | X | | | | |
| **McCarthy et al.** | **2004** | | X | | | |
| **Morana & Beltratti** | **2004** | | | | | X |
| **Matteo et al.** | **2004** | X | X | | | X |
| **Mulligan** | **2004** | X | | | | |
| **Mulligan & Lombardo** | **2004** | X | | | | |
| **Corazza & Malliaris** | **2002** | | | X | | X |
| **Henry & Olekalns** | **2002** | | | | | X |
| **Cheung & Lai** | **2001** | | | | | X |
| **Lee et al.** | **2001** | X | | | | |
| **Crato & Ray** | **2000** | | | X | | |
| **Grau-Carles** | **2000** | X | | | | |
| **Lien & Tse** | **1999** | X | | X | | |
| **Opong et al.** | **1999** | X | | | | |
| **Hauser** | **1998** | | | | X | |
| **Barkoulas & Baum** | **1998** | X | X | | | X |
| **Barkoulas et al.** | **1997** | | | | X | |
| **Jacobsen** | **1996** | X | | | | |
| **Cheung & Lai** | **1995** | X | | | | |
| **Evertsz** | **1995a,b** | X | | | | X |
| **Evertsz & Berkner** | **1995** | X | | | | |

Table 1: Studies of Long Memory Published in "A" Level Finance Journals Since 1994. (Source: Jamdee and Los, Working Paper, 2005)

# 8 Tables

| Models | | Properties |
|---|---|---|
| **Volatility Clustering, Martingale Pricing** | **Volatility Clustering, Arbitrage Opportunities** | |
| MMAR | FBM | **Long Memory Scale Consistency** |
| FIGARCH | ARFIMA | **Long Memory Scale Inconsistency** |
| GARCH | ARMA | **Short Memory Scale Inconsistency** |

Table 2: The Comparison Between MMAR And Other Time Series Models. Source: Mandelbrot, Fisher, and Calvet (1997) and Calvet and Fisher (2002).

| **Maturity** | **Pricing Hurst** ($H$) | **Trading Time Alpha Zero** ($\alpha_0$) | **Mean** ($\widehat{\lambda}$) | **Variance** ($\widehat{\sigma}^2$) |
|---|---|---|---|---|
| **10-Year** | 0.504 | 0.56 | 1.110 | 0.221 |
| **7-Year** | 0.516 | 0.57 | 1.104 | 0.208 |
| **5-Year** | 0.537 | 0.59 | 1.099 | 0.199 |
| **3-Year** | 0.548 | 0.61 | 1.113 | 0.226 |
| **2-Year** | 0.548 | 0.62 | 1.132 | 0.264 |
| **1-Year** | 0.568 | 0.64 | 1.127 | 0.253 |
| **6-Month** | 0.592 | 0.67 | 1.132 | 0.265 |
| **3-Month** | 0.572 | 0.66 | 1.153 | 0.306 |
| **Fed Funds** | 0.482 | 0.57 | 1.183 | 0.365 |

Table 3: The Parameters of Treasury Rate MMARs. Hurst is the monofractal Hurst Exponent of the empirical interest rate process. Alpha zero is the most probable Hurst exponent of the trading time's multifractal spectrum. Mean and variance are the first two moments of the lognormally distributed multinomial measures, respectively.

| **Maturity** | $c$ | $k$ | $a$ | $b$ |
|---|---|---|---|---|
| **10-Year** | -0.0002587 | 0.0000012 | 0.9434 | 0.0441 |
| **7-Year** | -0.000262 | 0.0000011 | 0.9444 | 0.0454 |
| **5-Year** | -0.0002326 | 0.0000015 | 0.9372 | 0.0515 |
| **3-Year** | -0.0002262 | 0.0000013 | 0.9367 | 0.0563 |
| **2-Year** | -0.0001589 | 0.0000015 | 0.9285 | 0.0643 |
| **1-Year** | -0.000026 | 0.0000012 | 0.9273 | 0.0694 |
| **6-Month** | 0.0000067 | 0.0000014 | 0.9069 | 0.091 |
| **3-Month** | 0.0002927 | 0.0000038 | 0.8362 | 0.1638 |
| **Fed Funds** | 0.0031 | 0.000627 | 0.2906 | 0.638 |

Table 4: The Parameters of GARCH(1,1). c is the coefficient of the constant term in mean equation. k is the coefficient of the constant term in the variance equation. a is the coefficient of the GARCH effect in the variance equation. b is the coefficient of the ARCH effect in the variance equation.

| Maturity | Average Hurst (MMAR) | Input Hurst (Empirical) |
|---|---|---|
| **10-Year** | 0.51 | 0.50 |
| **7-Year** | 0.52 | 0.52 |
| **5-Year** | 0.54 | 0.54 |
| **3-Year** | 0.55 | 0.55 |
| **2-Year** | 0.55 | 0.55 |
| **1-Year** | 0.57 | 0.57 |
| **6-Month** | 0.59 | 0.59 |
| **3-Month** | 0.57 | 0.57 |
| **Fed Funds** | 0.45 | 0.48 |

Table 5: Averaged Hurst Exponents of 1,000 Simulated MMARs. The average Hurst (MMAR) column provides the average of Hurst exponents from the 1,000 simulated MMARs for each maturity. The Input Hurst (Empirical) column shows the detected Hurst exponents from the empirical data for each maturity.

| | 10-Year | | | | 7-Year | | | |
|---|---|---|---|---|---|---|---|---|
| | | Mean $\tau(q)$ | | | | Mean $\tau(q)$ | | |
| **Moment (q)** | **Emp. Series** | **Sim. MMAR Cholesky** | **Sim. GBM** | **Sim. GARCH (1, 1)** | **Emp. Series** | **Sim. MMAR Cholesky** | **Sim. GBM** | **Sim. GARCH (1, 1)** |
| **1** | -0.47 | -0.45 | -0.50 | -0.50 | -0.46 | -0.44 | -0.50 | -0.50 |
| | | [-0.54,-0.37] | [-0.58, -0.41] | [-0.58, -0.41] | | [-0.55, -0.36] | [-0.57, -0.42] | [-0.58, -0.41] |
| **2** | 0.01 | 0.01 | 0.00 | 0.01 | 0.03 | 0.04 | 0.00 | 0.00 |
| | | [-0.20, 0.23] | [-0.16, 0.16] | [-0.17, 0.18] | | [-0.18, 0.21] | [-0.14, 0.16] | [-0.17, 0.20] |
| **3** | 0.44 | 0.41 | 0.49 | 0.50 | 0.47 | 0.45 | 0.50 | 0.50 |
| | | [-0.30, 0.88] | [0.23, 0.75] | [0.20, 0.82] | | [-0.15, 0.80] | [0.29, 0.74] | [0.21, 0.82] |
| **4** | 0.81 | 0.74 | 0.98 | 0.98 | 0.86 | 0.81 | 0.99 | 0.98 |
| | | [-0.08, 1.48] | [0.60, 1.35] | [0.52, 1.54] | | [-0.30, 1.40] | [0.69, 1.32] | [0.49, 1.54] |
| **5** | 1.13 | 1.04 | 1.47 | 1.44 | 1.21 | 1.14 | 1.48 | 1.44 |
| | | [-0.17, 2.02] | [0.94, 1.97] | [0.76, 2.25] | | [-0.49, 1.98] | [1.07, 1.98] | [0.68, 2.26] |
| | **5-Year** | | | | **3-Year** | | | |
| | | Mean $\tau(q)$ | | | | Mean $\tau(q)$ | | |
| **Moment (q)** | **Emp. Series** | **Sim. MMAR Cholesky** | **Sim. GBM** | **Sim. GARCH (1, 1)** | **Emp. Series** | **Sim. MMAR Cholesky** | **Sim. GBM** | **Sim. GARCH (1, 1)** |
| **1** | -0.44 | -0.43 | -0.50 | -0.50 | -0.42 | -0.41 | -0.50 | -0.50 |
| | | [-0.52, -0.33] | [-0.59, -0.43] | [-0.59, -0.43] | | [-0.48, -0.32] | [-0.59, -0.43] | [-0.58, -0.41] |
| **2** | 0.07 | 0.07 | 0.00 | 0.00 | 0.09 | 0.09 | 0.00 | 0.00 |
| | | [-0.17, 0.29] | [-0.14, 0.13] | [-0.19, 0.23] | | [-0.10, 0.29] | [-0.16, 0.15] | [-0.18, 0.20] |
| **3** | 0.52 | 0.51 | 0.50 | 0.49 | 0.52 | 0.50 | 0.50 | 0.48 |
| | | [0.05, 0.97] | [0.27, 0.70] | [0.18, 1.00] | | [0.11, 0.92] | [0.27, 0.72] | [0.07, 0.98] |
| **4** | 0.93 | 0.88 | 0.99 | 0.96 | 0.89 | 0.85 | 1.00 | 0.95 |
| | | [0.03, 1.60] | [0.66, 1.30] | [0.42, 1.76] | | [0.09, 1.52] | [0.68, 1.29] | [0.24, 1.83] |
| **5** | 1.30 | 1.22 | 1.48 | 1.42 | 1.21 | 1.15 | 1.49 | 1.39 |
| | | [-0.13, 2.20] | [1.04, 1.92] | [0.62, 2.47] | | [-0.03, 2.14] | [1.05, 1.91] | [0.38, 2.65] |

Table 6: The Comparison Between Scaling Exponents of Empirical Treasury Rates and Mean Scaling Exponents of Corresponding Simulated Processes. The results are for Treasury rates with longer than 2-year maturities. The first left column under each maturity provides the scaling exponents for the first five integer moments. The next three columns provide the average scaling exponents from 1,000 simulations for the MMAR, GBM, and GARCH(1,1) processes, respectively. The minimum and maximum values of the exponents are reported in parentheses. Emp. means 'Empirical' while Sim. means 'Simulated'.

| | 2-Year | | | | 1-Year | | | |
|---|---|---|---|---|---|---|---|---|
| | | Mean $\tau(q)$ | | | | Mean $\tau(q)$ | | |
| **Moment (q)** | **Emp. Series** | **Sim. MMAR Cholesky** | **Sim. GBM** | **Sim. GARCH (1,1)** | **Emp. Series** | **Sim. MMAR Cholesky** | **Sim. GBM** | **Sim. GARCH (1,1)** |
| **1** | -0.41 | -0.40 | -0.50 | -0.50 | -0.40 | -0.38 | -0.49 | -0.50 |
| | | [-0.48, -0.31] | [-0.58, -0.41] | [-0.61, -0.42] | | [-0.46,-0.29] | [-0.58,-0.42] | [-0.61, -0.42] |
| **2** | 0.09 | 0.09 | 0.01 | -0.01 | 0.13 | 0.13 | 0.01 | -0.01 |
| | | [-0.10, 0.33] | [-0.16, 0.16] | [-0.25, 0.19] | | [-0.10,0.32] | [-0.15,0.18] | [-0.27, 0.26] |
| **3** | 0.50 | 0.49 | 0.51 | 0.47 | 0.55 | 0.54 | 0.52 | 0.46 |
| | | [0.01, 1.01] | [0.25, 0.74] | [0.02, 0.89] | | [0.07,1.00] | [0.28,0.77] | [-0.01, 1.07] |
| **4** | 0.83 | 0.81 | 1.00 | 0.93 | 0.89 | 0.88 | 1.01 | 0.89 |
| | | [-0.11, 1.69] | [0.64, 1.32] | [0.20, 1.63] | | [0.05,1.58] | [0.71,1.35] | [0.08, 1.86] |
| **5** | 1.13 | 1.10 | 1.49 | 1.36 | 1.19 | 1.18 | 1.50 | 1.30 |
| | | [-0.22, 2.32] | [1.02, 1.94] | [0.35, 2.34] | | [-0.03,2.15] | [1.12,1.93] | [0.11, 2.60] |
| | **6-Month** | | | | **3-Month** | | | |
| | | Mean $\tau(q)$ | | | | Mean $\tau(q)$ | | |
| **Moment (q)** | **Emp. Series** | **Sim. MMAR Cholesky** | **Sim. GBM** | **Sim. GARCH (1,1)** | **Emp. Series** | **Sim. MMAR Cholesky** | **Sim. GBM** | **Sim. GARCH (1,1)** |
| **1** | -0.38 | -0.36 | -0.49 | -0.50 | -0.40 | -0.37 | -0.50 | -0.49 |
| | | [-0.44, -0.25] | [-0.59, -0.43] | [-0.58, -0.40] | | [-0.45, -0.27] | [-0.57, -0.43] | [-0.53, -0.47] |
| **2** | 0.17 | 0.16 | 0.01 | -0.01 | 0.14 | 0.13 | 0.01 | -0.01 |
| | | [-0.05, 0.43] | [-0.15, 0.15] | [-0.25, 0.32] | | [-0.13, 0.37] | [-0.16, 0.16] | [-0.27, 0.08] |
| **3** | 0.61 | 0.56 | 0.52 | 0.45 | 0.53 | 0.51 | 0.51 | 0.39 |
| | | [0.01, 1.11] | [0.25, 0.76] | [-0.07, 1.13] | | [-0.06, 1.08] | [0.24, 0.76] | [-0.14, 0.60] |
| **4** | 0.95 | 0.88 | 1.02 | 0.86 | 0.81 | 0.83 | 1.01 | 0.73 |
| | | [-0.04, 1.79] | [0.64, 1.38] | [0.02, 1.90] | | [-0.22, 1.77] | [0.64, 1.36] | [-0.05, 1.10] |
| **5** | 1.25 | 1.17 | 1.51 | 1.25 | 1.06 | 1.10 | 1.50 | 1.04 |
| | | [-0.15, 2.42] | [1.03, 1.99] | [0.09, 2.62] | | [-0.39, 2.42] | [1.03, 1.96] | [0.02, 1.58] |

Table 7: The Comparison Between Scaling Exponents of Empirical Treasury Rates and Mean Scaling Exponents of Corresponding Simulated Processes. The results are for Treasury rates with less than 3-year maturities. The first left column under each maturity provides the scaling exponents for the first five integer moments. The next three columns provide the average scaling exponents from 1,000 simulations for the MMAR, GBM, and GARCH(1,1) processes, respectively. The minimum and maximum values of the exponents are reported in parentheses. Emp. means 'Empirical' while Sim. means 'Simulated'.

| Fed Funds | | | |
|---|---|---|---|
| | Mean $\tau(q)$ | | |
| **Emp. Series** | **Sim. MMAR Cholesky** | **Sim. GBM** | **Sim. GARCH (1, 1)** |
| -0.46 | -0.5 | -0.51 | -0.41 |
| | [-0.62, -0.34] | [-0.64, -0.37] | [-0.59, -0.26] |
| -0.03 | -0.07 | -0.02 | 0.06 |
| | [-0.41, 0.23] | [-0.29, 0.22] | [-0.34, 0.31] |
| 0.3 | 0.29 | 0.46 | 0.37 |
| | [-0.53, 0.82] | [0.05, 0.84] | [-0.45, 0.83] |
| 0.56 | 0.58 | 0.92 | 0.59 |
| | [-0.76, 1.33] | [0.38, 1.45] | [-0.71, 1.35] |
| 0.79 | 0.84 | 1.37 | 0.78 |
| | [-1.00, 1.78] | [0.68, 2.07] | [-0.98, 1.84] |

Table 8: The Comparison Between Scaling Exponents of Empirical Fed Funds Rates and Mean Scaling Exponents of Corresponding Simulated Processes. The results are for Fed Funds rates. The first left column provides the scaling exponents for the first five integer moments. The next three columns provide the average scaling exponents from 1,000 simulations for the MMAR, GBM, and GARCH(1,1) processes, respectively. The minimum and maximum values of the exponents are reported in parentheses. Emp. means 'Empirical' while Sim. means 'Simulated'.